1 **Contribution of the Sensitivity Analysis in Groundwater Vulnerability ~~Assessing~~ Assessment Using the**

2 **DRASTIC and Composite DRASTIC Indexes**

3 Mohammad Malakootian[1], Majid Nozari[2]*

4 **Manuscript Authors details:**

5 1. Mohammad Malakootian, Department of Environmental Health, School of Public Health,

6 Kerman University of Medical Sciences, Iran. E-mail: m.malakootian@yahoo.com.

7 https://orcid.org/0000-0002-4051-6242.

8 2. Majid Nozari, Department of Environmental Health, School of Public Health, Kerman

9 University of Medical Sciences, Iran. Tel: 98-9383921819, E-mail: nozari.m@kmu.ac.ir.

10 https://orcid.org/0000-0003-2319-1930.

11

12

13

14

15

16

17

18

19

20

21

22

ABSTRACT

The present study estimates Kerman–Baghin aquifer vulnerability by applying the DRASTIC and composite DRASTIC (CDRASTIC) indexes. The factors affecting the transfer of contamination, including the water table depth, the soil media, the aquifer media, the impact of the vadose zone, the topography, the hydraulic conductivity, and the land use, were ranked, weighted, and integrated, using a geographical information system (GIS). A sensitivity test has also been performed to specify the sensitivity of the parameters. The study results show that the topographic layer displays a gentle slope in the aquifer. The majority of the aquifer covered irrigated field crops and grassland with a moderate vegetation cover. In addition, the aquifer vulnerability maps indicate very similar results, recognizing the northwest parts of the aquifer as areas with high and very high vulnerability. The map removal sensibility analysis (MRSA) revealed the impact of the vadose zone (in the DRASTIC index) and hydraulic conductivity (in the CDRASTIC index) as the most effective parameters in the vulnerability evaluation. In both indexes, the single-parameter sensibility analysis (SPSA) showed the net recharge as the most effective factor in the vulnerability estimation. From this study, it can be concluded that vulnerability maps can be used as a tool to control human activities for the sustained protection of aquifers.

1. Introduction

Groundwater is as a significant and principal freshwater resource in most parts of the world, especially for those in waterless and arid areas. Water quality has been given more emphasis on groundwater management (Neshat et al., 2014; Manap et al., 2013; Manap et al., 2014a; Ayazi et al., 2010). The potential groundwater's contamination by mankind operations at or near the surface of the groundwater has been supposed the major base for control of this source (Tilahun and Merkel, 2010).

The introduction of potential contaminants to a location on top of an aquifer at a specific location in an underground system is defined as groundwater vulnerability (Sarah and Patricia, 1993; Neshat et al., 2014). Groundwater vulnerability is an evaluation of the groundwater pollution relative hazard by a specific constituent. Vulnerability maps are commonly performed at a sub-basin, basin, or regional scale. They are not normally applied for site-specific evaluations including zones smaller than a few tens of square kilometers (Baalousha, 2006; Tilahun and Merkel, 2010). Different techniques have been presented to assess groundwater susceptibility with great precision (Javadi et al., 2010; Javadi et al., 2011). Mostly, these methods include analytic tools considered to relate groundwater contamination with land operations. There are three types of evaluation methods; the overlay and index; the process-based simulation and, the statistic procedures (Neshat et al., 2014; Dixon, 2004).

Overlay and index procedures affirm the incorporation of various zonal maps by allocating a numeral index. Both procedures are simple to use in the geographic information system, especially on a zonal measure. Hence, these methods are the most famous procedures applied to vulnerability estimation (Neshat et al., 2014). The most extensively used methods for the groundwater's vulnerability evaluation are GODS (Ghazavi and Ebrahimi, 2015), IRISH (Daly

and Drew, 1999), AVI (Raju et al., 2014), and DRASTIC (Neshat et al., 2014; Baghapour et al., 2014; Baghapour et al., 2016).

The DRASTIC index, ~~for the first time~~ proposed by Aller et al (1985), it is considered one of the best indexes for the groundwater vulnerability estimation. This method ignores the influences of zonal properties. Thus, identical weights and rating values are utilized. In addition, this technique does not apply a standard validation test for the aquifer. Therefore, several investigators developed this index using various techniques (Neshat et al., 2014). The higher DRASTIC index represents the greater contamination potential and inversely. After calculating the DRASTIC index, it should be possible to identify the zones that are more prone to pollution. This index only provides a relative estimation and is not created to make a complete assessment (Baalousha, 2006).

Many studies have been conducted using DRASTIC index to estimate the groundwater vulnerability in different regions of the world (Jaseela et al., 2016; Zghibi et al., 2016; Kardan Moghaddam et al., 2017; Kumar et al., 2016; Neshat and Pradhan, 2017; Souleymane and Tang, 2017; Ghosh and Kanchan, 2016; Saida et al., 2017), however, a fewer studies have used the CDRASTIC index for evaluation of the groundwater vulnerability (Baghapour et al., 2016; Baghapour et al., 2014; Secunda et al., 1998; Jayasekera et al., 2011; Shirazi et al., 2012; Jayasekera et al., 2008). Boughriba et al. (2010) utilized DRASTIC index in geographical information system environment for an estimation of the aquifer vulnerability. They provide the DRASTIC modified map prepared from total DRASTIC indexes and small monitoring network maps including two classes, high and medium. Then, authors integrated the map with the land use map to provide the contamination potential map. They reported that the new obtained groundwater vulnerability map including three various classes very high, high, and medium.

93   Babiker et al. (2005) used the DRASTIC index to determine prone points to contamination from

94   human activities in the aquifer. They reported that in terms of vulnerability, the western and

95   eastern parts of the aquifer fall in the high and medium classes, respectively. The final aquifer

96   vulnerability map represents that the high risk of pollution is in the eastern part of aquifer due to

97   agriculture activities. They also observed that the factor, net recharge has the biggest effect on

98   the aquifer vulnerability, followed by the soil media, the topography, the impact of the vadose

99   zone, and the hydraulic conductivity.

100   The water scarcity in Iran, with a mean annual rainfall about one-third of the world's annual

101   rainfall (Chitsazan and Akhtari, 2006; Modabberi et al., 2017) is a very critical and serious

102   problem. Also, the groundwater reduction makes worst the previous problem. Groundwater is the

103   only freshwater resource in the Kerman province, due to the lack of surface water. The aquifer,

104   object of this research, is located in the central part of Kerman province in Iran. Due to recent

105   droughts, this aquifer is placed under heavy pumping to irrigate crops, which cause gradually the

106   drop of the water level. Moreover, recently, the use of groundwater resources has been greater

107   than in former years. It makes the studies on the pathology and zoning the damages in

108   groundwater undeniable. Therefore, the purpose of this research is providing the Kerman-

109   Baghin aquifer vulnerability maps and performing the sensitivity analysis to identify the most

110   effective factors in the vulnerability assessment.

111   **2. Methodology**

112   **2.1. Study area**

113   The Kerman Province covers both semiarid and waterless areas. The present study included a

114   2023 km^2 area (29° 47′ to 30° 31′ N latitude and 56° 18′ to 57° 37′ E longitude) located in the

115   central part of the Kerman Province, Iran (Fig.1). The study area is mostly covered by

agricultural land (Neshat et al., 2014). In the study area, the mean annual rainfall is 108.3 mm (during 2017); the highest and lowest topographic elevation is 1,980 and 1,633 m above sea level; and eventually, the mean, minimum, and maximum annual temperatures are 17°C, -12°C, and 41°C, respectively (during 2017).
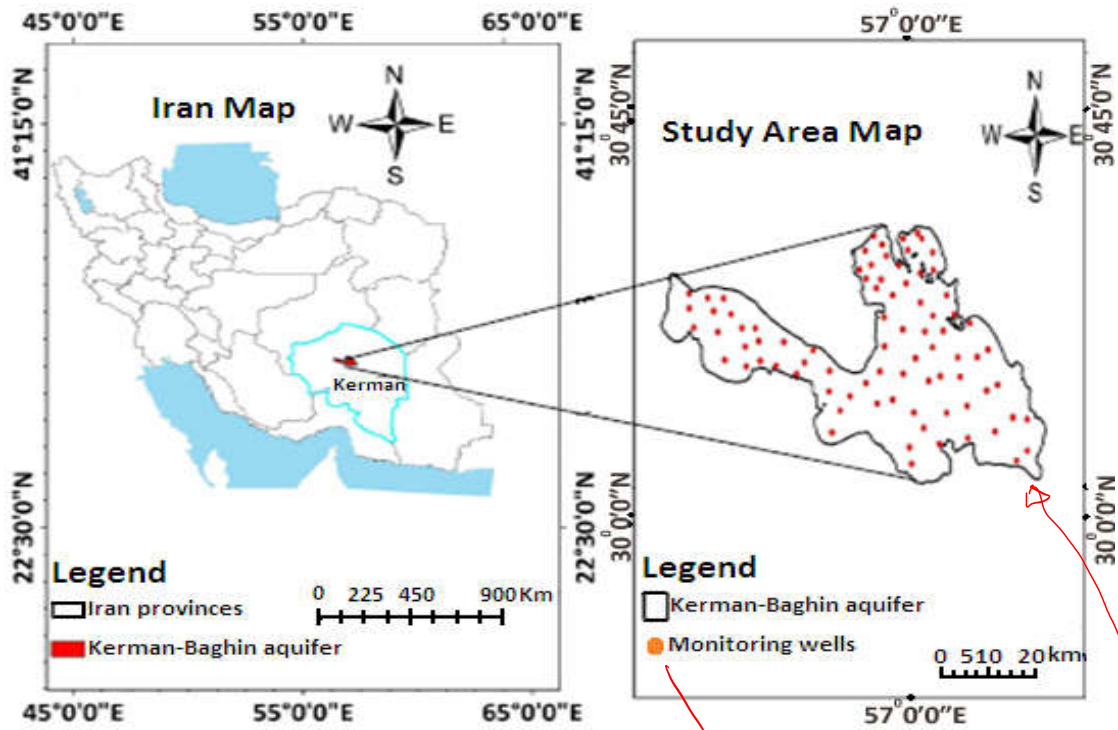
Fig. 1. Location map of the Kerman–Baghin aquifer *(handwritten: SHould THis be "red" color?)*

2.2. Computing the DRASTIC and CDRASTIC indexes

DRASTIC is a procedure developed by the United States Environmental Protection Agency (U.S EPA) to evaluate the groundwater pollution (Aller et al., 1985). A Higher DRASTIC index corresponds to a high vulnerability of the aquifer to pollution. Vulnerability ranges corresponding to the DRASTIC index are presented in Tab 1. In the DRASTIC index, each parameter is rated on a scale from 1 to 10 that shows the relative contamination potential of that parameter for that area. Also, in the DRASTIC index, one weight (1 to 5) is assigned to each of the parameters.

(handwritten: This part should appear after The definition of DRASTIC)

6

129 Weight values show the relative significance of the parameters with respect to each other. The

130 DRASTIC index is obtained using the following formula (Kardan Moghaddam et al., 2017;

131 Neshat and Pradhan, 2017):

132 $$\text{DRASTIC index} = D_r D_w + R_r R_w + A_r A_w + S_r S_w + T_r T_w + I_r I_w + C_r C_w. \tag{1}$$

133 In the above formula, the letters in the acronym DRASTIC comprise a short form of the effective

134 factors in the DRASTIC index. D, R, A, S, T, I, and C are the water table depth, the net recharge,

135 the aquifer media, the soil media, the topography, the impact of the vadose zone, and the

136 hydraulic conductivity, respectively. Also, "r" and "w" are the rating and weight of each factor,

137 respectively. The ratings and weights of the factors are depicted in Tab 2.

[handwritten margin note: How do you determine these values? Provide Supporting Material or Reference.]

138 **Table 1** The range of vulnerability related to the DRASTIC index

Vulnerability	Ranges
Very low	23-46
Low	47-92
Moderate	93-136
High	137-184
Very high	>185

139

140 **Table 2** Rating and weight-related to DRASTIC index factors

DRASTIC parameters	Range	Rating (r)	Weight (w)
Water table depth (m)	0.0-1.5	10	
	1.5-4.6	9	
	4.6-9.1	7	
	9.1-15.2	5	5
	15.2-22.9	3	
	22.9-30.5	2	
	>30.5	1	
Net recharge	11-13	10	
	9-11	8	
	7-9	5	4
	5-7	3	
	3-5	1	

7

Aquifer media	Rubble and sand	9	
	Gravel and sand	7	
	Gravel, sand, clay, and silt	5	3
	Sand and clay	4	
	Sand, clay, and silt	3	
Soil media	Rubble, sand, clay, and silt	9	
	Gravel and sand	7	
	Gravel, sand, clay, and silt	6	
	Sand	5	2
	Sand, clay, and silt	3	
	clay and silt	2	
Topography or slope (%)	0-2	10	
	2-6	9	
	6-12	5	1
	12-18	3	
	>18	1	
The impact of the vadose zone	Rubble, sand, clay, and silt	9	
	Gravel and sand	7	
	Gravel, sand, clay, and silt	5	5
	Sand, clay, and silt	3	
Hydraulic conductivity (m/day)	0-4.1	1	
	4.1-12.2	2	3
	12.2-28.5	4	
	28.5-40.7	6	
	40.7-81.5	8	

141

142   To get the CDRASTIC index, an additional factor (land use) is added to the above formula.

143   Thus, the CDRASTIC index was obtained as follows:

144     $$\text{CDRASTIC index} = D_r D_w + R_r R_w + A_r A_w + S_r S_w + T_r T_w + I_r I_w + C_r C_w + L_r L_w \qquad (2)$$

where

145 In the above formula, L_w and L_r are the relative weight and rating related to the land use factor,

146 respectively. Ratings and weightings applied to the pollution potential, which are related to the land

147 use factor based on the CDRASTIC index, are indicated in Tab 3. The CDRASTIC formula final

148 outputs are ranged from 28 to 280. Vulnerability ranges based on the CDRASTIC index are

149 presented in Tab 4.

150   **Table 3** Ratings and weighting applied to the pollution potential related to the land use factor

151   based on the CDRASTIC index How do you define the values?

8

Land use	Rating	Weight
Irrigated field crops + Urban areas	10	
Irrigated field crops + Grassland with poor vegetation cover + Urban areas	9	
Irrigated field crops + Grassland with moderate vegetation cover + Urban areas	8	
Irrigated field crops	8	
Irrigated field crops + Fallow land + Grassland with poor vegetation cover	7	
Irrigated field crops + Grassland with poor vegetation cover	7	
Irrigated field crops + Grassland with moderate vegetation cover	6	
Irrigated field crops + Rocky + Urban areas	5	5
Irrigated field crops + Grassland with poor vegetation cover + Woodland	5	
Irrigated field crops + Woodland	5	
Irrigated field crops + Rocky	4	
Fallow land	3	
Fallow land + Grassland with poor vegetation cover	3	
Fallow land + Grassland with moderate vegetation cover	3	
Grassland with poor vegetation cover	2	
Grassland with moderate vegetation cover	2	
Grassland with moderate vegetation cover + Woodland	1	
Sand dune +Grassland with moderate vegetation cover	1	
Sand dune	1	

152

153 **Table 4** Vulnerability ranges related to the CDRASTIC index

Vulnerability	Ranges
Very low	<100
Low	100-145
Moderate	145-190
High	190-235
Very high	≥235

154 **2.3. Water table depth**

155 The water table depth factor is the distance of water table from the Earth's surface, in a well

156 (Baghapour et al., 2016). 83 wells in the Kerman–Baghin aquifer were utilized to obtain this

157 factor. The interpolation procedure was used to provide a raster map of the water table depth

158 factor, which was categorized based on Tab 2.

159 **2.4. Net recharge**

9

160 Net recharge is the amount of runoff that permeates into the ground and reaches the groundwater

161 surface (Singh et al., 2015; Ghosh and Kanchan, 2016). This research uses the Piscopo method

162 (Chitsazan and Akhtari, 2009) to provide the net recharge layer for the Kerman–Baghin aquifer

163 according to the following equation and Tab 5:

164 $$\text{Net recharge factor} = \text{slope (\%)} + \text{rainfall} + \text{soil permeability}. \tag{3}$$

165 In the above equation, the percentage of slope was calculated from a topographical map, using a

166 digital elevation model. Also, a soil permeability map was created using the Kerman–Baghin

167 aquifer soil map (with scale 1:250000) and the drilling logs of the 83 wells. In the end, a map of

168 the area's rainfall rate was compiled based on the annual average precipitation. Ratings and

169 weights of the net recharge factor are illustrated in Tab 5.

170 **Table 5** Weight, rating, and range of the net recharge parameter

Slope (%)		Rainfall		Soil permeability		Net Recharge		
Range (%)	Factor	Range (mm/year)	Factor	Range	Factor	Range (cm/year)	Rating	Weight
<2	4	>850	4	High	5	11-13	10	
2-10	3	700-850	3	Moderate to high	4	9-11	8	
10-33	2	500-700	2	Moderate	3	7-9	5	4
>33	1	<500	1	Low	2	5-7	3	
				Very low	1	3-5	1	

171 **2.5. Aquifer media**

172 Aquifer media parameter controls the path of groundwater streams in the aquifer (Aller et al.,

173 1985; Singh et al., 2015). To obtain this layer, the 83 well's drilling log data were used. The data

174 were gathered from the Kerman Regional Water Office (KRWO). The range of the aquifer media

175 layer is shown in Tab 2.

176 **2.6. Soil media**

177 The soil media has a considerable effect on the amount of water surface that can penetrate into

178 the aquifer. Therefore, where the soil layer is thick, the debilitation processes such as absorption,

179 filtration, degradation, and evaporation may be considerable (Singh et al., 2015). A soil media

180 raster map was provided using the Kerman–Baghin aquifer soil map and the well's drilling logs.

181 **2.7. Topography**

182 The topography controls the residence time of water inside on the soil and the degree of

183 penetration (Singh et al., 2015). For obtain this layer, the percentage of the slope was provided

184 from the topographical map, using a digital elevation model. The data were gathered from the

185 KRWO. The range of the topographic layer is presented in Tab 2.

186 **2.8. The impact of the vadose zone**

187 The vadose zone is the unsaturated area located between the topographic surface and the

188 groundwater level (Singh et al., 2015). It plays a considerable role in decreasing groundwater

189 contamination by pollutant debilitation processes such as purification, chemical reaction, and

190 dispersal (Shirazi et al., 2012). In order to prepare this layer, the wells drilling log data were

191 used. The data were gathered from the KRWO. The impact range of the vadose zone layer is

192 depicted in Tab 2.

193 **2.9. Hydraulic conductivity**

194 The hydraulic conductivity refers to the capability of the aquifer to transfer water. The high

195 hydraulic conductivity areas demonstrate a high potential for groundwater contamination (Singh

196 et al., 2015; Aller et al., 1985). To prepare this layer, data derived from pumping tests of wells

197 were used. The range of the hydraulic conductivity layer is shown in Tab 2.

198 **2.10. Land use**

Land use influences groundwater resources via variation in recharge amount and by changing freshwater demands for water. Land use is obligatory since it is required by the CDRASTIC index. The Indian remote sensing satellite information was utilized to providing land use raster map. The weight and rating related to the land use layer are presented in Tab 3.

2.11. Sensitivity Analyses

One of the main advantages of the DRASTIC index is the evaluation performance because of high number of input data are used, this allows to restrict the effects of errors on the final results. Nevertheless, some investigators, like Babiker et al. (2005), Barber et al. (1993), and Merchant (1994), reported that similar results could be obtained using fewer data and lower costs. The unavoidable subjectivity related to the choice of the seven factors, ranks, and weights utilized to calculate the vulnerability index has also been criticized. Therefore, in order to eliminate the aforementioned criticisms, two sensitivity analyses were performed as follows (Napolitano and Fabbri, 1996):

A. Map removal sensibility analysis (MRSA)

MRSA value indicates the vulnerability map sensibility to removal one or more maps from the suitability analysis. MRSA is calculated as follows (Babiker et al., 2005; Martínez-Bastida et al., 2010; Saidi et al., 2011; Modabberi et al., 2017):

$$S = \left[\left| \frac{\frac{V}{N} - \frac{V'}{n}}{V} \right| \right] \times 100 \tag{4}$$

S is the sensibility value expressed in terms of variation index, V is the intrinsic vulnerability index (real vulnerability index) and V′ is the intrinsic vulnerability index after removal of factor

219   X, N and n are the numbers of data factors utilized to calculate V and V', respectively (Babiker et

220   al., 2005; Martínez-Bastida et al., 2010; Saidi et al., 2011; Modabberi et al., 2017).

221   **B. Single-parameter sensibility analysis (SPSA)**

222   SPSA was presented by Napolitano and Fabbri (1996) for the first time. This test shows the

223   effect of each of the DRASTIC factors in the final vulnerability index. Using this test derived

224   from equation 5, the real and effective weight of each factor, compared to the theoretical weight

225   assigned by the analytical model was calculated (Babiker et al., 2005; Martínez-Bastida et al.,

226   2010; Saidi et al., 2011; Modabberi et al., 2017),

227    $$W = \left[\frac{P_r P_w}{V}\right] \times 100 \qquad (5)$$

228   Where, W is the effective weight of each factor. P_r and P_w are the rank and weight assigned to

229   factor P, respectively. V is the intrinsic vulnerability index (Martínez-Bastida et al., 2010;

230   Babiker et al., 2005; Saidi et al., 2011; Modabberi et al., 2017).

231   **3. Results and discussion**

232   **3.1. DRASTIC and CDRASTIC parameters**

233   Based on the data shown in Tab 2, the assigned rating of water table depth varies from 1 to 10. In

234   addition, based on the results presented in Tab 6, the water table depth in the aquifer varies from

235   4.6 to >30.5 m (rating 1 to 7). Around 27.55% of the aquifer has a depth greater than 30.5 m, and

236   66.16 % of the aquifer has a depth ranging from 9.1 m and 30.5 m. Less than 7% has a depth

237   between 4.6 m and 9.1 m. The Kerman–Baghin aquifer rated map of water table depth factor is

238   presented in Fig 2(A). According to Fig 2(A) and Tab 6, the minimum impact of the water table

239   depth parameter on aquifer vulnerability occurs in the central parts (6.39%), whereas the

240   maximum impact occurs in the north, south, northwest, and southeast parts (27.55%).

13

241   According to the results presented in Tab 6, 75.81% of the aquifer has a net recharge value in

242   the range of 7 to 9 cm/year. 11.74% of the aquifer has a net recharge value between 9 and 11

243   cm/year. The Kerman–Baghin aquifer rated map of the net recharge parameter is shown in Fig

244   2(B). According to Piscopo's method, the Kerman–Baghin aquifer was divided into three classes,

245   with regards to the net recharge factor. The highest net recharge value was seen in the north,

246   northeast, south, southwest, parts of the northwest, parts of the center, and parts of the southeast

247   (75.81%), whereas the least net recharge value appeared in parts of the northwest and center

248   (11.74%), as shown in Fig 2(B) and Tab 6.

249   As observed in Tab 6, the majority of the Kerman–Baghin aquifer media is composed of sand,

250   clay, and silt (75.21%). The Kerman–Baghin aquifer rated map of aquifer media is presented in

251   Fig 3(A). Parts of the aquifer in the north, northwest, northeast, center, and southeast are

252   composed of sand, clay, and silt. Parts of the aquifer in the northwest are composed of rubble and

253   sand (5.58%). Parts of the aquifer in the south and northwest are composed of gravel and sand

254   (8.95%), and gravel, sand, clay, and silt (10.26%).

255   The Kerman–Baghin aquifer rated map of the soil media parameter is presented in Fig 3(B).

256   The soil map depicts six different classes of the soil. The highest rank (rank = 9) was assigned to

257   rubble, sand, clay, and silt (a combination of rubble, sand, clay and silt soils). Also, the lowest

258   rank (rank = 2) was assigned to clay and silt (a combination of clay and silt soils). Most of the

259   aquifer soil media is covered with silt, sand, and clay (about 80%).

260   The Kerman–Baghin aquifer rated map of the topography parameter is indicated in Fig 4(A).

261   The topographical layer shows a gentle slope (0 to 6%) over most of the aquifer, hence gaining

262   ranks of 9 and 10. A slope range of 0 to 2% includes 34.72% of the study area, and its rating

263   (slope range = 0–2%) is 10. Also, 65.28% of the aquifer has a slope range of 2 to 6% (parts of

the northwest) as shown in Fig 4(A) and Tab 6. As the gradient increases, the runoff increases as well (Israil et al., 2006) leading to less penetration (Jaiswal et al., 2003). Based on Madrucci et al. (2008), the gradients higher than 35° are considered restrictions on groundwater desirability because of the lack of springs.

The Kerman–Baghin aquifer rated map of the impact of the vadose zone parameter is indicated in Fig 4(B). According to the results, the soil with a rank of 5 (gravel, sand, clay, and silt) is more effective on aquifer vulnerability (35.47%). Other various types of soils such as sand, clay, and silt (parts of the north, northeast, south, and southeast), gravel and sand (parts of the center and northwest), and rubble, sand, clay, and silt (parts of the northwest) cover 34.24%, 20.39%, and 9.9% of the aquifer, respectively, as shown in Fig 4(B) and Tab 6. Sandy soil is effective on groundwater occurrence because of the high rate of penetration (Srivastava and Bhattacharya, 2006). However, clay soil is arranged poorly because of the low infiltration (Manap et al., 2014b).

The Kerman–Baghin aquifer rated map of the hydraulic conductivity parameter is presented in Fig 5(A). The hydraulic conductivity factor shows high variability. Our study results show that the hydraulic conductivity parameter of the Kerman–Baghin aquifer varied from 0 to 81.5 m/day. The potential for groundwater contamination greater in zones with high hydraulic conductivity (38.27%). As shown in Fig 5(A) and Tab 6, 29.51%, 23.93%, 5.98%, and 2.31% of the study areas have hydraulic conductivity in the ranges of 0 to 4.1 m/day, 12.2 to 28.5 m/day, 28.5 to 40.7 m/day, and 40.7 to 81.5 m/day, respectively.

The Kerman–Baghin aquifer rated map of the land use parameter is presented in Fig 5(B). Our results show that the majority of the Kerman–Baghin aquifer is covered with irrigated field crops and grassland with moderate vegetation cover (20.45%). Less than 4% of the study area is

287   irrigated field crops and urban areas (3.61%), and 58.47% ==of the== study area is irrigated field

288   crops with urban areas, grassland with poor and moderate vegetation cover, fallow land,

289   woodland, and rocky ground. In addition, 10.17% ==of the study== area is fallow land with poor

290   grassland and moderate vegetation cover, and 13.72% ==of the study== area is sand dunes with poor

291   grassland and moderate vegetation cover and woodland as shown in ==Fig== 5(B) and ==Tabs== 3 and 6.
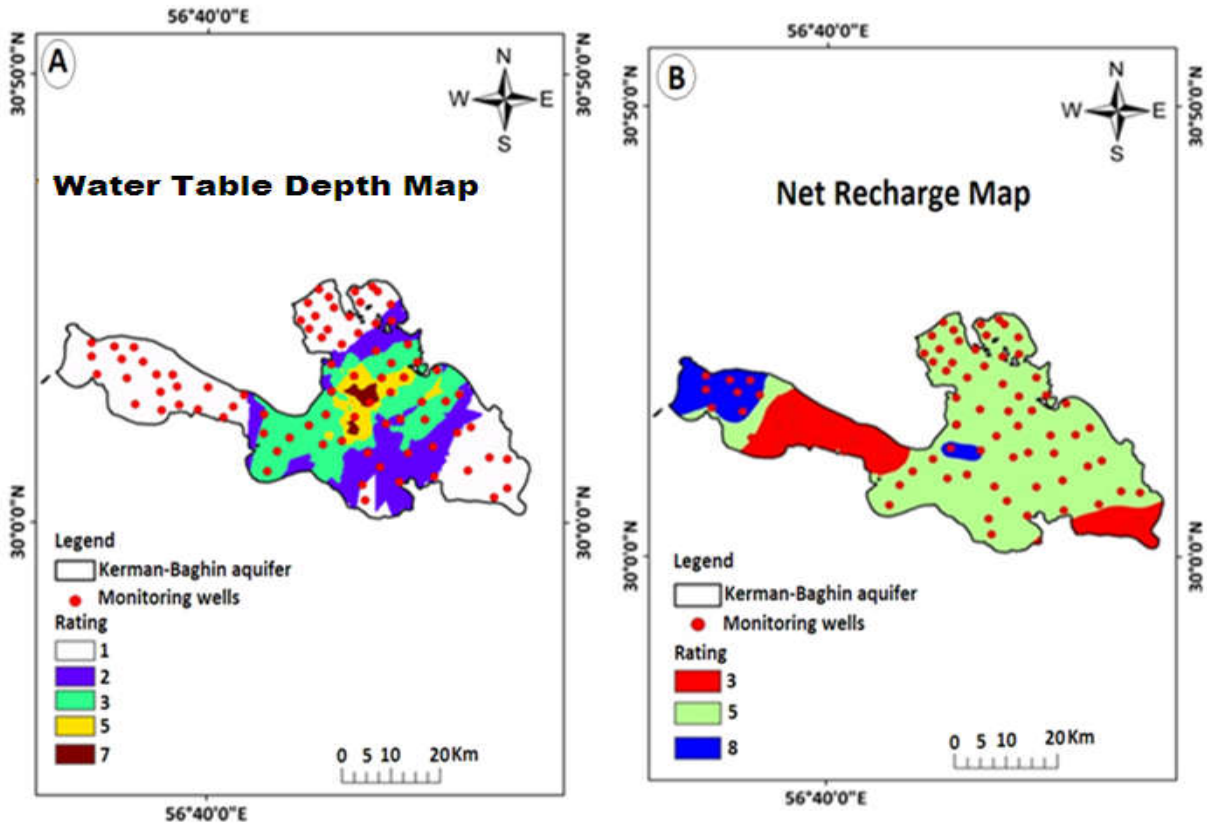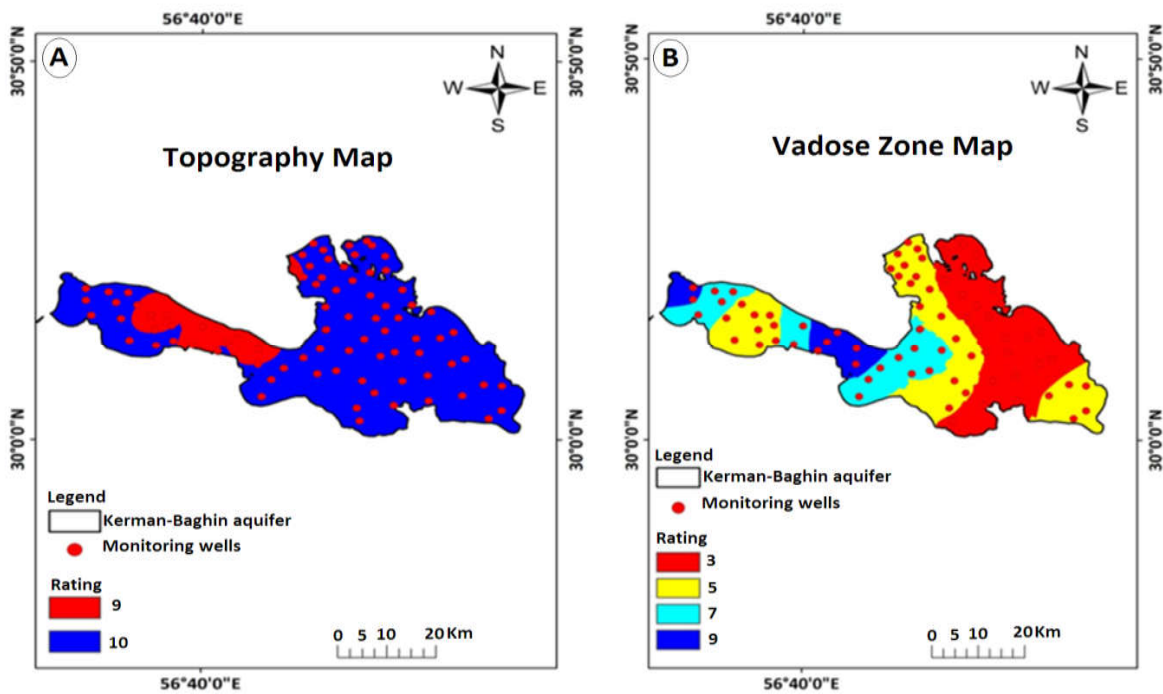

292

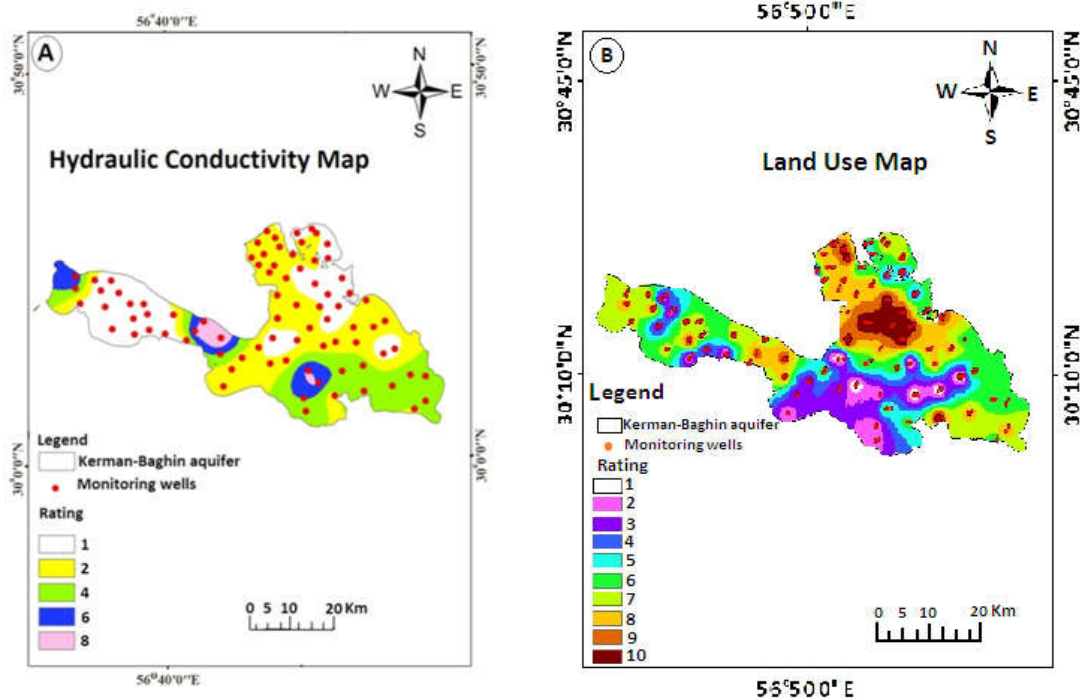293   **Fig. 2.** Kerman–Baghin aquifer rated maps of A) water table depth and B) net recharge

16

294
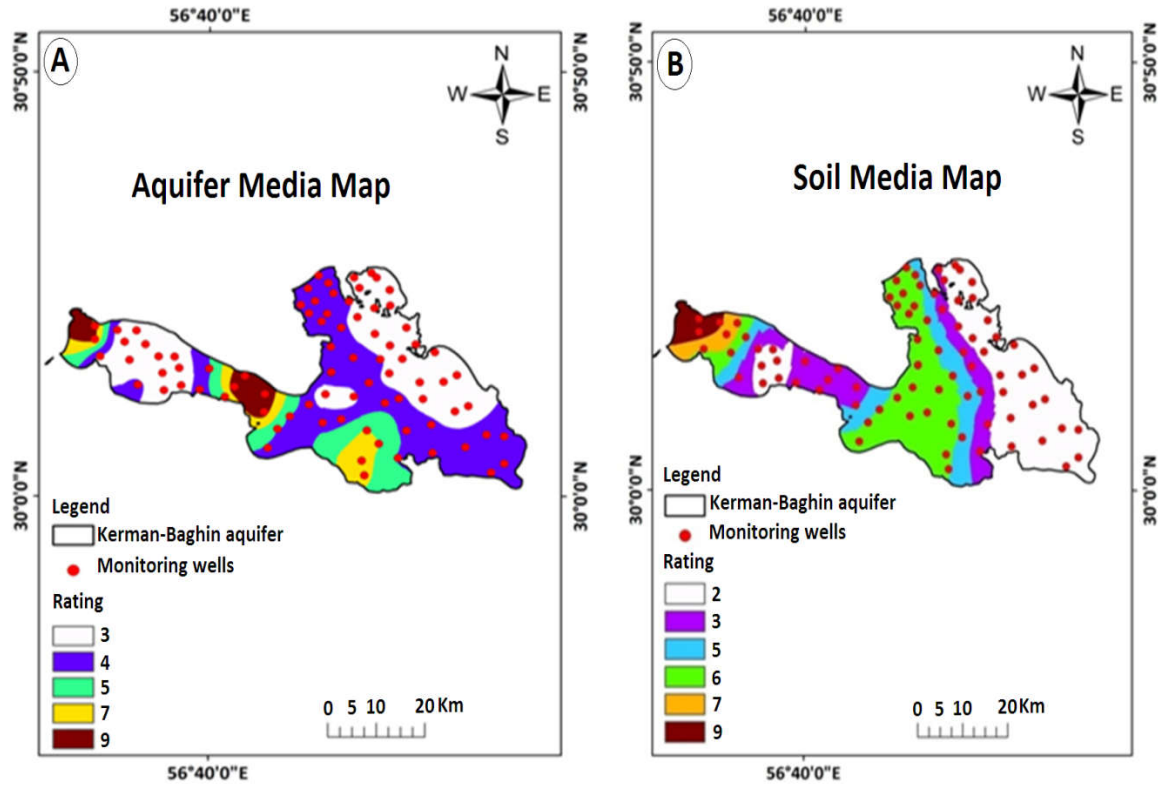
Fig. 3. Kerman–Baghin aquifer rated maps of A) aquifer media and B) soil media

296

Fig. 4. Kerman–Baghin aquifer rated maps of A) topography and B) vadose zone

17

298

Fig. 5. Kerman–Baghin aquifer rated maps of A) hydraulic conductivity and B) land use

**Table 6** The area of rating (km² and %) of the DRASTIC and CDRASTIC parameters

DRASTIC and CDRASTIC indexes parameters	Rating	Area (km²)	Area (%)	The aquifer geographic directions covered by the respective rating in the parameters rated maps
Water table depth	1	557.73	27.55	Parts of the north, south, northwest, and southeast
	2	472.18	23.34	Parts of the north, south, and center
	3	469.78	23.29	Parts of the center
	5	395.00	19.53	Parts of the center
	7	129.14	6.39	Parts of the center
Net recharge	3	252.04	12.45	Parts of southeast, and northwest
	5	1534.15	75.81	North, northeast, south, southwest, and parts of the northwest, center, southeast
	8	237.6	11.74	Parts of the northwest and center
Aquifer media	3	743.18	36.72	Parts of the north, northwest, northeast, and center
	4	779.01	38.49	Parts of the north, northwest, southeast, and center
	5	207.81	10.26	Parts of the south, and northwest
	7	181.02	8.95	Parts of the south, and northwest
	9	112.76	5.58	Parts of the northwest
Soil media	2	658.5	32.53	Parts of the north, northwest, northeast, and southeast
	3	399.72	19.75	Parts of the north, northwest, south, and center

18

	5	297.44	14.69	Parts of the north, northwest, south, and center
	6	538.77	26.62	Parts of the northwest, center, and southwest
	7	67.56	3.33	Parts of the northwest
	9	61.79	3.08	Parts of the northwest
Topography	9	702.74	34.72	North, northwest, northeast, south, southeast, southwest, and center
	10	1321.07	65.28	parts of the northwest
The impact of the vadose zone	3	692.87	34.24	Parts of the north, northeast, south, and southeast
	5	717.91	35.47	Parts of the north, northwest, south, southeast, and center
	7	412.49	20.39	Parts of the center, and northwest
	9	200.53	9.9	Parts of the northwest
Hydraulic conductivity	1	597.11	29.51	Parts of the northeast, northwest, southeast, and center
	2	774.52	38.27	parts of the northwest, south, southeast, and center
	4	484.17	23.93	Parts of the northwest, south, and southeast
	6	120.99	5.98	Parts of the south, and northwest
	8	46.7	2.31	Parts of the south, and northwest
Land use	1	112.48	5.56	Parts of the south
	2	165.02	8.16	Parts of the south
	3	205.65	10.17	Parts of the south, and center
	4	357.06	17.64	Parts of the south, southwest, northwest, and center
	5	234.86	11.61	Parts of the southeast, northwest, and center
	6	413.86	20.45	Parts of the southeast, northwest, northeast, and center
	7	182.63	9.02	Parts of the north, northwest, and northeast
	8	169.4	8.37	Parts of the north, northwest, and northeast
	9	109.42	5.41	Parts of the north, northwest, and northeast
	10	73.09	3.61	Parts of the north

3.2. DRASTIC and CDRASTIC vulnerability indexes

301

302 The Kerman–Baghin aquifer vulnerability map using DRASTIC and CDRASTIC indexes is

303 shown in Fig 6. In the studied aquifer, the vulnerability falls under very high, high, moderate,

304 low, and very low vulnerable areas. It is found that in both indexes, the parts of north, northeast,

305 northwest, south, southwest, southeast and center come under low and very low vulnerability.

306 This can be attributed to low water depth, hydraulic conductivity, and net recharge characterizing

19

307 these aquifer areas; an other reason might be that the aquifer media mostly are mostly clay, sand

308 and silt soils. The area of the vulnerability, identified by investigated indexes, is illustrated in

309 Tab 7. Low and very low vulnerable zones cover 25.21% and 38.31%, respectively, of the

310 Kerman–Baghin aquifer using the DRASTIC index. Very low and low vulnerable zones cover

311 24.95% and 40.41%, respectively, using the CDRASTIC index. This is primarily due to water

312 table depth and relatively low permeability of the vadose zone in such aquifers (Colins et al.,

313 2016). Around 26 % of the studied aquifer has moderate groundwater pollution potential, using

314 DRASTIC and CDRASTIC indexes. This does not mean that such areas are without pollution

315 but it is relatively prone to pollution when compared with other areas (Colins et al., 2016). From

316 the DRASTIC index values, it was noticed that 10.4% of the study aquifer is under high (8.46%)

317 and very high (1.94%) vulnerability. The results of the study showed that 8.75% of the aquifer is

318 in the ranges of 190 to 235 and greater than 235 in the CDRASTIC index (Tab 7). The

319 vulnerability maps according to these two indexes indicated very same findings, showing the

320 northwest portion of the aquifer as the high and very high vulnerable zones. The high

321 vulnerability can be attributed to great water depth, hydraulic conductivity, and net recharge in

322 these aquifer areas. In addition, this can due to the great slope in this area.
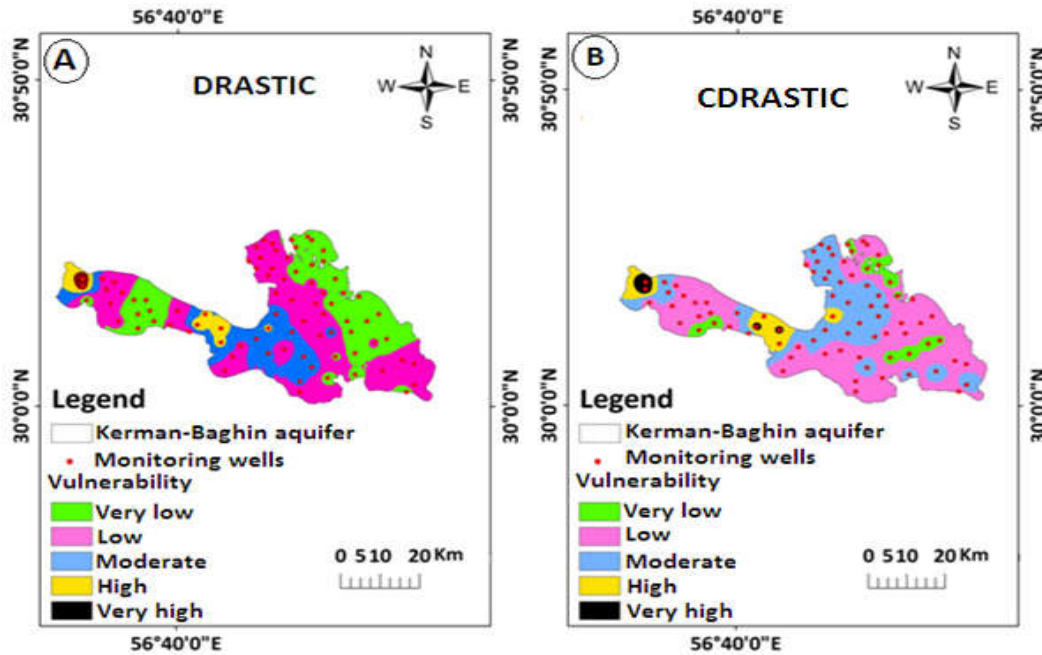
Fig. 6. The vulnerability maps of the Kerman–Baghin aquifer by DRASTIC and CDRASTIC indexes

Table 7 The area of vulnerability (km^2 and %) identified by DRASTIC and CDRASTIC indexes

Vulnerability	DRASTIC				CDRASTIC			
	Ranges	Area (km^2)	Area (%)	The aquifer geographic directions covered by the respective vulnerability	Ranges	Area (km^2)	Area (%)	The aquifer geographic directions covered by the respective vulnerability
Very low	23-46	510.25	25.21	Parts of the south, north, northwest, and northeast	<100	505.02	24.95	Parts of the southeast, north, northwest, and northeast
Low	47-92	775.14	38.31	Parts of the south, southwest, southeast, north, northwest, northeast, and center	100-145	817.70	40.41	Parts of the south, southwest, southeast, north, northwest, northeast, and center
Moderate	93-136	527.85	26.08	Parts of the south, southwest, northwest, and center	145-190	524.06	25.89	Parts of the south, southwest, southwest, northwest, and center
High	137-184	171.02	8.46	Parts of the northwest	190-235	126.91	6.28	Parts of the northwest and center
Very high	>185	39.23	1.94	Parts of the northwest	≥235	49.79	2.47	Parts of the northwest

3.3. The sensitivity of the DRASTIC model

The MRSA, the DRASTIC index, is performed by eliminating one layer data at a time as indicated in Tab 8. The results showed a high variation in vulnerability index when the impact of

21

the vadose zone factor was removed, so that, the average variation index is 1.88%. This shows that this factor is more effective in vulnerability assessment using the DRASTIC index. When this parameter is removed from the overlay process, this leads to a significant decrease in vulnerability index. This could be due to the high theoretical weight assigned to this factor (weight = 5). These findings are similar to those obtained by Dibi et al. (2012) who have shown that, in addition to this parameter, topography, net recharge, and water table depth have a high impact on the vulnerability index. Also, in Samake et al. (2011), the impact of the vadose zone and the hydraulic conductivity parameters had a considerable impact on the vulnerability index, that appears to have a moderate sensitivity to the deletion of water table depth (1.48%), net recharge (1.36%), and hydraulic conductivity (1.25%) parameters. The minimum menu variation index was achieved after eliminating the aquifer media factor (0.44%), as indicated in Tab 8.

For the estimation of the individual factors effect towards aquifer vulnerability, the SPSA is performed. The results summaries of SPSA in the DRASTIC index are shown in Tab 9. The SPSA compares the effective weights and theoretical weights. The average value of the effective weight of the net recharge factor is 43.26% and its theoretical weight (%) is 17.4%. This shows that this factor is more effective in vulnerability assessment using the DRASTIC index. The results reported by other studies (Babiker et al., 2005; Doumouya et al., 2012) are similar to those of the present study. The impact of the vadose zone and water table depth parameters has high theoretical weights (21.74%); they have been dedicated with an effective weight with average value such as 8.33% and 25.55%. The remaining factors show an average value of the effective weights of 14.91% (aquifer media), 9.89% (soil media), 11.35% (topography), and 7.01% (hydraulic conductivity). The theoretical weights assigned to the water table depth, net recharge, topography, and hydraulic conductivity parameters are not in agreement with the

354 effective weight. The highest and lowest impact on aquifer vulnerability was related to the net

355 recharge and hydraulic conductivity parameters, respectively (Tab 9).

356 **Table 8** Statistical results of MRSA in the DRASTIC index

The sensitivity of variability index (S) (%)				Removed parameters
SD	Min.	Max.	Ave.	
0.414	0.05	2.36	1.36	D
0.775	0.07	3.06	1.48	R
0.311	0.05	1.31	0.44	A
0.486	0.00	1.65	0.73	S
0.339	0.03	1.31	0.51	T
0.894	0.25	3.84	1.88	I
0.550	0.03	1.98	1.25	C

357

358 **Table 9** Statistical results of SPSA in the DRASTIC index

Effective weight (%)				Theoretical weight (%)	Theoretical weight	Parameters
SD	Min.	Max.	Ave.			
6.179	3.23	28.46	8.33	21.74	5	D
11.998	14.06	73.47	43.26	17.4	4	R
3.190	7.26	22.13	14.91	13.04	3	A
2.916	4.49	14.29	9. 89	8.7	2	S
2.222	6.45	14.71	11.35	4.3	1	T
5.367	15.79	37.31	25.55	21.74	5	I
3.738	2.42	18.75	7.01	13.04	3	C

359

3.4. The sensibility of the CDRASTIC index

361 The MRSA in the CDRASTIC index is performed by eliminating on data layer at a time as

362 indicated in Tab 10. The mean variation index of hydraulic conductivity parameter is 4.13%. The

363 hydraulic conductivity has a greater effect on the aquifer vulnerability followed by water table

364 depth (4.05%), soil media (3.82%), topography (3.68%), aquifer media (3.28%), net recharge

365 (2.72%), the impact of the vadose zone (2.33%), and land use (1.99%).

366 The effective weight derived from the SPSA to the CDRASTIC index is shown in Tab 11.

367 The average value of the effective weight of the net recharge factor is 32.62%. This shows that

368 this factor is more effective in vulnerability assessment using CDRASTIC index. The hydraulic

369 conductivity displays the lowest effective weights (5.32%). The topography, net recharge, and

370 land use had upper effective weights toward the theoretical weights specified by CDRASTIC

371 index. The average value of the effective weight of the land use parameter is 24.82%. This shows

372 that this parameter is the second effective parameter in aquifer vulnerability, using the

373 CDRASTIC index (Tab 11).

374 **Table 10** Statistical results of MRSA in the CDRASTIC index

The sensitivity of variability index (S) (%)				Removed parameters
SD	Min.	Max.	Ave.	
1.403	0.50	6.48	4.05	D
1.617	0.11	10.91	2.72	R
1.541	0.06	5.99	3.28	A
1.508	0.67	6.60	3.82	S
1.353	0.87	5.87	3.68	T
1.439	0.06	5.12	2.33	I
1.480	0.55	6.72	4.13	C
0.375	1.23	3.00	1.99	L

375

376 **Table 11** Statistical results of SPSA in the CDRASTIC index

Effective weight (%)				Theoretical weight (%)	Theoretical weight	Parameters
SD	Min.	Max.	Ave.			
4.849	2.63	26.88	6.27	21.74	5	D
10.672	10.4	66.67	32.62	17.4	4	R
3.026	6.29	20.00	11.23	13.04	3	A
2.621	3.31	12.96	7.5	8.7	2	S
1.609	5.2	12.82	8.45	4.3	1	T
4.648	10.87	32.05	19.2	21.74	5	I
3.134	2.1	14.88	5.32	13.04	3	C
10.122	3.88	42.37	24.82	17.85	5	L

377

378 **4. Conclusions**

379 Evaluations of vulnerability indexes for the Kerman–Baghin aquifer were conducted using the

380 GIS-based DRASTIC and CDRASTIC indexes. Seven hydro–geological factors (the letters

381 comprising the acronym) are applied to determine aquifer vulnerability with DRASTIC; eight

382 hydro–geological parameters (one additional to the seven in DRASTIC) with the CDRASTIC

24

Approach

383 ~~index~~. From the DRASTIC index values, it was determined that 10.4% of the aquifer is under

384 high (8.46%) ~~and~~ *to* very high (1.94%) vulnerability. From the CDRASTIC index values, it was

385 determined that 8.75% of the aquifer is under high (6.28%) ~~and~~ *to* very high (2.47%) vulnerability.

386 Also, we found that parts of the north, south, southeast, and northwest ~~are under~~ *have* low ~~and~~ *to* very

387 low vulnerability ~~using~~ *based on* the DRASTIC and CDRASTIC indexes. Agricultural and industrial *No support for this — Conclusion*

388 activities ~~are found~~ *were thought* to be ~~a~~ major threat*s* in the zones with high ~~and~~ *to* very high vulnerability. The

389 MRSA signifies the fact that hydraulic conductivity and the impact of the vadose zone ~~factors~~

390 induce a high risk of aquifer contamination according to the DRASTIC and CDRASTIC indexes,

391 respectively. ~~In~~ *for methods* both ~~indexes~~, the SPSA analysis shows the net recharge ~~factor as~~ *has* a high risk for

392 aquifer contamination. These results indicate that the studied indexes are effective tools for *How? You did not validate the analysis*

393 determining groundwater vulnerability. Also, these results could be utilized by private and

394 government agencies as a guide for groundwater contamination assessment in Iran.

Acknowledgments

Competing interests. The authors declare that they have no conflict of interest.

References

Aller, L., Truman, b., Jay H, L., Rebeeca J, P., and Glen, H.: DRASTIC: a standardized system

for evaluating ground water pollution potential using hydrogeologic settings, U.S Environmental

Protection Agency, USA, 1985.

Ayazi, M. H., Pirasteh, S., Arvin, A., Pradhan, B., Nikouravan, B., and Mansor, S.: Disasters and risk reduction in groundwater: Zagros Mountain Southwest Iran using geoinformatics techniques, Disaster Adv., 3, 51-57, 2010.

Baalousha, H.: Vulnerability assessment for the Gaza Strip, Palestine using DRASTIC, J. Environ. Geol., 50, 405-414, https://doi.org/10.1007/s00254-006-0219-z, 2006.

Babiker, I. S., Mohamed, M. A., Hiyama, T., and Kato, K.: A GIS-based DRASTIC model for assessing aquifer vulnerability in Kakamigahara Heights, Gifu Prefecture, central Japan, Sci Total Environ., 345, 127-140, https://doi.org/10.1016/j.scitotenv.2004.11.005, 2005.

Baghapour, M. A., Talebbeydokhti, N., Tabatabee, H., and Nobandegani, A. F.: Assessment of groundwater nitrate pollution and determination of groundwater protection zones using DRASTIC and composite DRASTIC (CD) models: the case of Shiraz unconfined aquifer, J. Health. Sci. Surveill. Syst., 2, 54-65, 2014.

Baghapour, M. A., Nobandegani, A. F., Talebbeydokhti, N., Bagherzadeh, S., Nadiri, A. A., Gharekhani, M., and Chitsazan, N.: Optimization of DRASTIC method by artificial neural network, nitrate vulnerability index, and composite DRASTIC models to assess groundwater vulnerability for unconfined aquifer of Shiraz Plain, Iran, J Environ Health Sci Eng., 14, 1-16, https://doi.org/10.1186/s40201-016-0254-y, 2016.

Barber, C., Bates, L. E., Barron, R., and Allison, H.: Assessment of the relative vulnerability of groundwater to pollution: a review and background paper for the conference workshop on vulnerability assessment, AGSO J Aust Geol Geophys., 14, 147-154, 1993.

Boughriba, M., Barkaoui, A.-e., Zarhloule, Y., Lahmer, Z., El Houadi, B., and Verdoya, M.: Groundwater vulnerability and risk mapping of the Angad transboundary aquifer using

425 DRASTIC index method in GIS environment, Arab J Geosci., 3, 207-220,

426 https://doi.org/10.1007/s12517-009-0072-y, 2010.

427 Chitsazan, M., and Akhtari, Y.: Evaluating the potential of groundwater pollution in Kherran and

428 Zoweircherry plains through GIS-based DRASTIC model, J. Water. Wastewater, 17, 39-51,

429 2006.

430 Chitsazan, M., and Akhtari, Y.: A GIS-based DRASTIC model for assessing aquifer

431 vulnerability in Kherran Plain, Khuzestan, Iran, Water Resour Manag., 23, 1137-1155,

432 https://doi.org/10.1007/s11269-008-9319-8, 2009.

433 Colins, J., Sashikkumar, M., Anas, P., and Kirubakaran, M.: GIS-based assessment of aquifer

434 vulnerability using DRASTIC Model: A case study on Kodaganar basin, Earth Sci. Res. J., 20, 1-

435 8, https://doi.org/10.15446/esrj.v20n1.52469, 2016.

436 Daly, D., and Drew, D.: Irish methodologies for karst aquifer protection, in: Beek B (ed)

437 Hydrogeology and engineering geology of sinkholes and karst, Balkema, Rotterdam, 267-272,

438 1999.

439 Dibi, B., Kouame, K. I., Konan-Waidhet, A. B., Savane, I., Biemi, J., Nedeff, V., and Lazar, G.:

440 Impact of agriculture on the quality of groundwater resources in peri-urban zone of Songon

441 (Cote D'ivoire), Environ. Engine. Manage. J., 11, 2173-2182,

442 https://doi.org/10.30638/eemj.2012.271, 2012.

443 Dixon, B.: Prediction of ground water vulnerability using an integrated GIS-based Neuro-Fuzzy

444 techniques, J. Spat. Hydro., 4, 1-38, 2004.

445 Doumouya, I., Dibi, B., Kouame, K. I., Saley, B., Jourda, J. P., Savane, I., and Biemi, J.:

446 Modelling of favourable zones for the establishment of water points by geographical information

447   system (GIS) and multicriteria analysis (MCA) in the Aboisso area (South-east of Côte d'Ivoire),

448   Environ. Earth. Sci., 67, 1763-1780, https://doi.org/10.1007/s12665-012-1622-2, 2012.

449   Ghazavi, R., and Ebrahimi, Z.: Assessing groundwater vulnerability to contamination in an arid

450   environment using DRASTIC and GOD models, Inte. J. Environ. Sci. Tech, 12, 2909-2918,

451   https://doi.org/10.1007/s13762-015-0813-2, 2015.

452   Ghosh, T., and Kanchan, R.: Aquifer vulnerability assessment in the Bengal alluvial tract, India,

453   using GIS based DRASTIC model, Model Earth Syst Environ., 2, 2-13,

454   https://doi.org/10.1007/s40808-016-0208-5, 2016.

455   Israil, M., Al-hadithi, M., Singhal, D., Kumar, B., Rao, M. S., and Verma, S.: Groundwater

456   resources evaluation in the Piedmont zone of Himalaya, India, using Isotope and GIS techniques,

457   J. Spatial. Hydro., 6, 107-119, 2006.

458   Jaiswal, R., Mukherjee, S., Krishnamurthy, J., and Saxena, R.: Role of remote sensing and GIS

459   techniques for generation of groundwater prospect zones towards rural development--an

460   approach, Int J Remote Sens., 24, 993-1008, https://doi.org/10.1080/01431160210144543, 2003.

461   Jaseela, C., Prabhakar, K., and Harikumar, P. S. P.: Application of GIS and DRASTIC modeling

462   for evaluation of groundwater vulnerability near a solid waste disposal site, Int. J. Geoscien., 7,

463   558-571, https://doi.org/10.4236/ijg.2016.74043, 2016.

464   Javadi, S., Kavehkar, N., Mousavizadeh, M., and Mohammadi, K.: Modification of DRASTIC

465   model to map groundwater vulnerability to pollution using nitrate measurements in agricultural

466   areas, J. Agr. Sci. Tech., 13, 239-249, 2010.

467   Javadi, S., Kavehkar, N., Mohammadi, K., Khodadadi, A., and Kahawita, R.: Calibrating

468   DRASTIC using field measurements, sensitivity analysis and statistical methods to assess

groundwater vulnerability, Water. Int., 36, 719-732, https://doi.org/10.1080/02508060.2011.610921, 2011.

Jayasekera, D., Kaluarachchi, J. J., and Villholth, K. G.: Groundwater Quality Impacts Due to Population Growth and Land Use Exploitation in the Coastal Aquifers of Sri Lanka, Southern Illinois University Carbondale 2008, 43.

Jayasekera, D. L., Kaluarachchi, J. J., and Villholth, K. G.: Groundwater stress and vulnerability in rural coastal aquifers under competing demands: a case study from Sri Lanka, Environ Monit Assess. , 176, 13-30, https://doi.org/10.1007/s10661-010-1563-8, 2011.

Kardan Moghaddam, H., Jafari, F., and Javadi, S.: Vulnerability evaluation of a coastal aquifer via GALDIT model and comparison with DRASTIC index using quality parameters, Hydro. Sci. J., 62, 137-146, https://doi.org/10.1080/02626667.2015.1080827, 2017.

Kumar, P., Thakur, P. K., Bansod, B. K., and Debnath, S. K.: Assessment of the effectiveness of DRASTIC in predicting the vulnerability of groundwater to contamination: a case study from Fatehgarh Sahib district in Punjab, India, Environ. Earth. Sci., 75, 879, https://doi.org/10.1007/s12665-016-5712-4, 2016.

Madrucci, V., Taioli, F., and de Araújo, C. C.: Groundwater favorability map using GIS multicriteria data analysis on crystalline terrain, Sao Paulo State, Brazil, J. Hydro., 357, 153-173, https://doi.org/10.1016/j.jhydrol.2008.03.026, 2008.

Manap, M. A., Sulaiman, W. N. A., Ramli, M. F., Pradhan, B., and Surip, N.: A knowledge-driven GIS modeling technique for groundwater potential mapping at the Upper Langat Basin, Malaysia, Arabian. J. Geosci., 6, 1621-1637, https://doi.org/10.1007/s12517-011-0469-2, 2013.

Manap, M. A., Nampak, H., Pradhan, B., Lee, S., Sulaiman, W. N. A., and Ramli, M. F.: Application of probabilistic-based frequency ratio model in groundwater potential mapping using

492   remote sensing data and GIS, Arabian. J.Geosci., 7, 711-724, https://doi.org/10.1007/s12517-

493   012-0795-z, 2014a.

494   Manap, M. A., Nampak, H., Pradhan, B., Lee, S., Sulaiman, W. N. A., and Ramli, M. F.:

495   Application of probabilistic-based frequency ratio model in groundwater potential mapping using

496   remote sensing data and GIS, Arabian. J. Geosci., 7, 711-724, https://doi.org/10.1007/s12517-

497   012-0795-z, 2014b.

498   Martínez-Bastida, J. J., Arauzo, M., and Valladolid, M.: Intrinsic and specific vulnerability of

499   groundwater in central Spain: the risk of nitrate pollution, Hydro. J., 18, 681-698,

500   https://doi.org/10.1007/s10040-009-0549-5, 2010.

501   Merchant, J. W.: GIS-based groundwater pollution hazard assessment: a critical review of the

502   DRASTIC model, Photogramm Eng Remote Sensing., 60, 1117-1127, 1994.

503   Modabberi, H., Hashemi, M. M. R., Ashournia, M., and Rahimipour, M. A.: Sensitivity Analysis

504   and Vulnerability Mapping of the Guilan Aquifer Using Drastic Method, Rev. Environ. Earth.

505   Sci., 4, 27-41, https://doi.org/10.18488/journal.80.2017.41.27.41, 2017.

506   Napolitano, P., and Fabbri, A.: Single-parameter sensitivity analysis for aquifer vulnerability

507   assessment using DRASTIC and SINTACS, Proceedings of the Vienna Conference,

508   Netherlands, 1996, 559-566,

509   Neshat, A., Pradhan, B., Pirasteh, S., and Shafri, H. Z. M.: Estimating groundwater vulnerability

510   to pollution using a modified DRASTIC model in the Kerman agricultural area, Iran, Environ.

511   Earth. Sci., 71, 3119-3131, https://doi.org/10.1007/s12665-013-2690-7, 2014.

512   Neshat, A., and Pradhan, B.: Evaluation of groundwater vulnerability to pollution using

513   DRASTIC framework and GIS, Arabian. J. Geosci., 10, 2-8, https://doi.org/10.1007/s12517-017-

514   3292-6, 2017.

515 Raju, N. J., Ram, P., and Gossel, W.: Evaluation of groundwater vulnerability in the lower

516 Varuna catchment area, Uttar Pradesh, India using AVI concept, J. Geol. Soc. India., 83, 273-

517 278, https://doi.org/10.1007/s12594-014-0039-9, 2014.

518 Saida, S., Tarik, H., Abdellah, A., Farid, H., and Hakim, B.: Assessment of groundwater

519 vulnerability to nitrate based on the optimised DRASTIC models in the GIS Environment (Case

520 of Sidi Rached Basin, Algeria), Geosciences, 7, 2-23,

521 https://doi.org/10.3390/geosciences7020020, 2017.

522 Saidi, S., Bouri, S., and Ben Dhia, H.: Sensitivity analysis in groundwater vulnerability

523 assessment based on GIS in the Mahdia-Ksour Essaf aquifer, Tunisia: a validation study, Hydro.

524 Sci. J., 56, 288-304, https://doi.org/10.1080/02626667.2011.552886, 2011.

525 Samake, M., Tang, Z., Hlaing, W., Mbue, I. N., Kasereka, K., and Balogun, W. O.: Groundwater

526 vulnerability assessment in shallow aquifer in Linfen Basin, Shanxi Province, China using

527 DRASTIC model, J. Sustain. Develop., 4, 53-71, https://doi.org/10.5539/jsd.v4n1p53, 2011.

528 Sarah, C., and Patricia l, C.: Ground water vulnerability assessment: Predicting relative

529 contamination potential under conditions of uncertainty, National Academies Press, USA, 1993.

530 Secunda, S., Collin, M., and Melloul, A. J.: Groundwater vulnerability assessment using a

531 composite model combining DRASTIC with extensive agricultural land use in Israel's Sharon

532 region, J. Environ. Manage., 54, 39-57, https://doi.org/10.1006/jema.1998.0221, 1998.

533 Shirazi, S. M., Imran, H., and Akib, S.: GIS-based DRASTIC method for groundwater

534 vulnerability assessment: a review, J. Risk. Res., 15, 991-1011,

535 https://doi.org/10.1080/13669877.2012.686053, 2012.

536 Singh, A., Srivastav, S., Kumar, S., and Chakrapani, G. J.: A modified-DRASTIC model

537 (DRASTICA) for assessment of groundwater vulnerability to pollution in an urbanized

538   environment in Lucknow, India, Environ. Earth. Sci., 74, 5475-5490,

539   https://doi.org/10.1007/s12665-015-4558-5, 2015.

540   Souleymane, K., and Tang, Z.: A novel method of sensitivity analysis testing by applying the

541   DRASTIC and fuzzy optimization methods to assess groundwater vulnerability to pollution: the

542   case of the Senegal River basin in Mali, Nat. Hazards. Earth. Sys. Sci., 17, 1375-1392,

543   https://doi.org/10.5194/nhess-17-1375-2017, 2017.

544   Srivastava, P. K., and Bhattacharya, A. K.: Groundwater assessment through an integrated

545   approach using remote sensing, GIS and resistivity techniques: a case study from a hard rock

546   terrain, Int. J. Remote. Sens., 27, 4599-4620, https://doi.org/10.1080/01431160600554983,

547   2006.

548   Tilahun, K., and Merkel, B. J.: Assessment of groundwater vulnerability to pollution in Dire

549   Dawa, Ethiopia using DRASTIC, Environ. Earth. Sci., 59, 1485-1496,

550   https://doi.org/10.1007/s12665-009-0134-1, 2010.

551   Zghibi, A., Merzougui, A., Chenini, I., Ergaieg, K., Zouhri, L., and Tarhouni, J.: Groundwater

552   vulnerability analysis of Tunisian coastal aquifer: an application of DRASTIC index method in

553   GIS environment, Groundwater. Sustain. Develop., 2, 169-181,

554   https://doi.org/10.1016/j.gsd.2016.10.001, 2016.

555